Optimal Home Energy Management under Hybrid PV-Storage Uncertainty: A Distributionally Robust Chance-Constrained Approach

Pengfei Zhao[1], Han Wu[2], Chenghong Gu[1*], Ignacio Hernando-Gil[3]

[1] Department of Electronic and Electrical Engineering, University of Bath, Bath, United Kingdom
[2] The College of Energy and Electrical Engineering, Hohai University, Nanjing, China
[3] ESTIA Institute of Technology, University of Bordeaux, F-64210 Bidart, France.
[*]C.Gu@bath.ac.uk

Abstract: Energy storage and demand response resources, in combination with intermittent renewable generation, are expected to provide domestic customers with the capability of reducing their electricity consumption. This paper highlights the role that an intelligent battery control, in combination with solar generation, could play to increase renewable uptake while reducing customers' electricity bills without intruding on people's daily life. The optimal performance of a home energy management system (HEMS) is investigated through a range of demand-response (DR) interventions, leading to different levels of customer weariness and consumption patterns. Thus, DR is applied with efficient and specific control of domestic appliances through load shifting and curtailment. Regarding the uncertainty associated with PV generation, a chance-constrained (CC) optimal scheduling is considered subject to the operation constraints from each power component in the HEMS. By applying distributionally robust optimization (DRO), the ambiguity set is accurately built for this distributionally robust chance-constrained (DRCC) problem without the need of any probability distribution associated with uncertainty. Based on the greatly altered consumption profiles in this paper, the proposed DRCC-HEMS is proven to be optimally effective and computationally efficient while considering uncertainty.

Nomenclature

A. Sets

$\mathcal{T}$	Set of time slots.
$\mathcal{A}$	Set of appliances.

B. Parameters

F	Fuse capacity.
$\underline{P}^{ESS,c}$, $\underline{P}^{ESS,d}$	Minimum charging and discharging power of ESS.
$\overline{P}^{ESS,c}$, $\overline{P}^{ESS,d}$	Maximum charging and discharging power of ESS.
$\underline{SOC}$, $\overline{SOC}$	Minimum and maximum state of charge of ESS.
$\eta^{ESS,c}$, $\eta^{ESS,d}$	Charging and discharging efficiency of ESS.
$C^{ESS,unit}$	Degradation cost coefficient of ESS.
$C^{ESS,cap}$, L^{ESS}, $E^{ESS,total}$	Capital cost, life cycle and total capacity of ESS.
$\underline{P^b}$, $\overline{P^b}$	Minimum and maximum power purchase from grid.
$C^b(t)$	Unit power purchase cost.
$\omega^f(t)$	PV output forecast.
$R^{re}(t)$, $R^{sh}(t)$	Reward when implementing load reduction and shifting.
$\underline{\Delta P_a^{re}}(t)$, $\underline{\Delta P_a^{sh}}(t)$	Minimum load reduction and shifting of appliance a at time t.
$\overline{\Delta P_a^{re}}(t)$, $\overline{\Delta P_a^{sh}}(t)$	Maximum load reduction and shifting of appliance a at time t.
$\varphi_a^{re}(t)$, $\varphi_a^{sh}(t)$	Weariness level for load reduction and shifting of appliance a at time t.
λ^{DR}	Weighting factor for weariness objective.

C. Decision variables

$P_a(t)$	Power consumption of each appliance at time t.
$u^{ESS,c}(t)$, $u^{ESS,d}(t)$	Status for charging and discharging power of ESS at time t.
$P^{ESS,c}(t)$, $P^{ESS,d}(t)$	Charging and discharging power of ESS at time t.
$SOC(t)$	State of charge of ESS at time t.
$E^{ESS}(t)$	Remaining capacity of ESS at time t
$C^{ESS,total}$	The total operation cost in the entire day.
$P^b(t)$	Power of buying electricity at time t.
$C^{b,Total}$	Cost of buying electricity.
$\omega^s(t)$	Scheduled PV output at time t.
$\Delta P_a^{re}(t)$, $\Delta P_a^{sh}(t)$	Load reduction and shifting of appliance a at time t compared with no DR implementation.
G^{DR}	Benefit of implementing DR.

D. Uncertainty

ϵ_i	Violation probability of chance constraint i.
$\xi(t)$	Uncertain PV forecast error at time t.
μ_0	Statistical mean of ξ.
Γ_0	Statistical covariance of ξ.

1. Introduction

Due to the current development of renewable energy (RE), control and communication technologies, domestic electricity consumers can increasingly benefit from a more efficient and cost-effective energy usage. Within this context, home energy management systems (HEMS), comprised of small-scale power components, are suitable for applying individual residential services and enabling significant bill reductions through an efficient power component scheduling [1, 2]. A typical HEMS structure consists of an energy storage system (ESS), RE generation of different types and scales, and communication technologies. Other than the optimal scheduling of power supplies through HEMS, energy cost reductions can also be achieved through demand response (DR), providing ways of altering the consumption profile applied by consumers. Based on DR incentive policies, both load curtailment and load shifting can be implemented [3]. More specifically, price-based DR is operated based on different pricing schemes such as time of use (TOU) and real-time pricing (RTP) tariffs [4]. Incentive-based DR also involves a higher rate of customer participation when reasonable penalty and rewards are provided [5]. For example, in [6], priorities of DR on appliances are set according to customer preferences, where simulation analysis is thus carried out to validate its applicability. Following this line of research, Chen et al evaluate a real-time price-based DR for home appliances considering the price uncertainty developed by robust optimization (RO) and stochastic optimization [7]. Moreover, in [8], a monthly bill target is optimized considering comfort level through a price-based DR with a multi-day time horizon.

However, the introduction of intermittent RE within the HEMS will result in an inaccurate output forecast, affecting the optimal scheduling and control of other system units. Accordingly, the uncertainty caused by renewable generation (RG) needs to be considered carefully, which is mainly addressed by RO and chance-constrained programming (CCP) in the wider literature.

On the one hand, RO strictly ensures there are no constraint violations within the boundary of the uncertainty set. In RO, the uncertainty is treated as uncertain variables bounded within the uncertainty set, without the association with any probability distribution. Particularly, in [9] and [10], the uncertainty in RG, load and market price has been investigated by the application of RO on HEMS. A more realistic model, considering specific home appliances, is also investigated to minimize the cost of electricity for a smart home in [11], which is designed for residential services only. However, restricting the analysis to the worst-case scenario will inevitably lead to conservative results.

On the other hand, another common approach for modelling uncertainty is CCP, which ensures a constraint is satisfied under a predefined probability. On this research topic, Liu et al investigated two grid-connected microgrids by the application of CCP, while considering an output restriction from RG within a specific confidence level. The problem is thus formulated as a linear programming case in [12]. Other examples of the latest use of CCP include [13], where the optimal scheduling of a combined heat and power (CHP) microgrid is handled by CCP and solved by particle swarm optimization (PSO). In [14], both PSO and two-point estimate methods are used to solve chance-constrained (CC) HEMS with DR. Accordingly, CCP either requires a large number of samples to approximate the uncertainty distribution, which is practically challenging and computationally demanding, or assumes a specific distribution based on historical data, which is over-optimistic. Beta distribution has been widely used to model the output probability from the intermittent photovoltaic (PV) generation. However, it can be considered as a forcing approach, and impractical to estimate accurately.

Based on all previous considerations, distributionally robust optimization (DRO) considers no assumption of uncertainty distribution, which only requires limited statistical data such as moment information. Previous research in power systems has shown that DRO outperforms RO and CCP in terms of less conservatism and weakened assumption on specifying uncertainty distributions [15-17]. With DRO, the ambiguity set is constructed by statistical information to restricting possible distributions, such as moment information [18, 19]. Based on more valuable distribution information, further research finds that the best estimate of the distribution can be obtained through the statistical fitting. Accordingly, statistical distance information can be added in the ambiguity set and thus the size of the ambiguity set can be controlled [20, 21]. Reference [15] proposes a DRO model for economic dispatch in a two-stage scheme. A two-stage unit commitment considering wind uncertainty is proposed in [16] by using DRO method. Reference [22] proposes a distributionally robust optimal gas-power flow in the sense of Wasserstein distance. Kullback-Leibler divergence is utilized in [23] to measure the distance between distributions in a unit commitment problem.

DRO can also be used to approximate CCP and therefore distributionally robust chance-constrained programming (DRCCP) is formed, requiring no exact uncertainty distribution. As of the same feature than CCP, DRCCP allows a permittable violation of certain constraints under a specific confidence interval, and the reformulation is always tractable. Compared with RO, DRCCP considers the worst distribution rather than the worst-case scenario, thus to address the conservativeness [18]. Compared to CCP, only specific and limited information is needed in DRCCP, which only requires statistical data such as moment information, with no need for an exact uncertainty distribution. For example, in [24], an energy management CC problem for an islanded microgrid is presented by considering uncertain RG and variable demand. In that case, the demand analysis is reformulated by DRO as a second order conic programming (SOCP) problem with mean and variance moment information, where the unique box-type ambiguity set is used to specify a box region for moment information with bounds. Also, in [25], an optimal power flow analysis is approximated in terms of a two-sided chance constrained set, but still a SOCP reformulation is made. Finally, both semi-definite

programming (SDP) and SOCP reformulations are yielded in [26], where two innovative DRCCP approaches are compared with two traditional CCP approaches.

In this paper, the DRCCP method is directly applied to the HEMS with respect to solar energy uncertainty, which also incorporates DR participation by customers. To describe the relative inconvenience and tiredness caused by DR to electricity consumers, instead of using the frequent term 'dissatisfaction' which is commonly used by power utilities, the term 'weariness' is defined in this paper [27]. The frequently used 'inconvenience' or 'dissatisfaction' is not appropriate to describe the volunteering DR in this paper, because these two terms are normally used to evaluate the impact associated with utilities [27, 28]. However, the scope of this paper is not on utility side, but only considers the over participation in DR, which will result in 'weariness' on DR. Accordingly, the proposed distributionally robust chance-constraint home energy management system (DRCC-HEMS) approach will benefit electricity users by realistically considering the RG within home energy systems. This approach further improves deterministic optimization techniques, as these do not consider the uncertainty arising from RG, and thus optimistically consider the generation output to be certain without any variation. The ambiguity set of DRCCP is given by mean values and the covariance matrix of uncertain variables, and thus the DRCC-HEMS is reformulated in this paper as a SOCP problem using Chebyshev's inequality method. The main contributions of this paper are:

i. Compared to work [2, 8, 14] which develops HEMS without considering DR, this paper proposes a new optimization framework considering DR benefit function, which can reflect the impact on end customers regarding customer's comfort and weariness due to participation;
ii. It for the first time proposes a novel DRCC-HEMS. Compared to CC-HEMS that requires a large amount of PV usage information [12-14], DRCC-HEMS has the advantages of: 1) being less data dependent through using moment information, which avoids violating the extensive PV usage privacy of customers; and 2) being higher computational efficiency with less data required.
iii. Compared to traditional robust HEMS which usess deterministic uncertainty sets [9-11] that would produce very conservative decisions, DRCC-HEMS is capable of capturing distributional information to mitigate the conservativity and thus is more cost effective for end customers.
iv. The novel DRCC-HEMS can help customers to use electricity wisely and economically through an optimal appliance load scheduling, an optimal ESS dispatch, and energy purchase scheme.

The rest of the paper is structured as follows: Section 2 proposes the mathematical modelling of the HEMS appliances, PV generation and ESS. Section 3 proposes the expression of DR and operation strategies. DRCCP and its associated reformulation is proposed in section 4. In section 5, the performance of DRCC-HEMS is evaluated on demand changing, daily expected operation cost and computation time, plus a comparison is made by CC-HEMS.

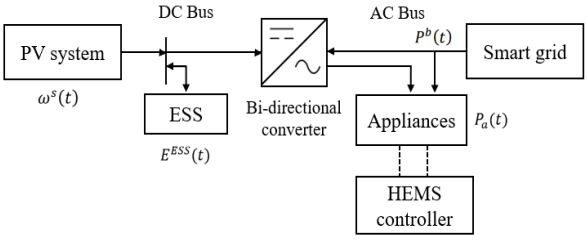

Fig. 1. *Schematic diagram of HEMS*

2. HEMS Modelling

The HEMS proposed in this paper contains ESS, PV and different types of loads categorized for DR. Through controlling each power component at every single time slot, the comprehensive objective incorporating both operation cost and weariness can be achieved. Time is discretized into 1, 2, . . . , 48 as $\mathcal{T}$ for every half hour. Accordingly, the appliance demand is grouped as set $\mathcal{A}$.

2.1. Domestic Home Appliances

If an efficient DR is to be implemented, a general load representation cannot be directly used to represent all types of domestic appliances. This is mainly due to: (i) not all the appliances are suitable for DR, (ii) the unique electric characteristic of each appliance is different, (iii) users have different preferences for each appliance. Thus, the aggregated general load should be decomposed into different load categories based on their electrical characteristics. The DR implementation incorporates load shifting and reduction which will inevitably create a 'weariness' of customers to some extent by DR actions. For the analysis in this paper, the typical consumption from the domestic load sector in the UK [29] is divided into 9 different categories (top up heating and storage heating are combined into storage heating which have similar characteristics): (a) consumer electronics, (b) cooking, (c) wet loads, (d) cold loads, (e) storage domestic hot water (DHW), (f) direct DHW, (g) direct heating, (h) storage heating and (i) lighting.

2.1.1 Critical and Cold Loads: The domestic load considered 'critical' in this paper consists of consumer electronics, cooking and lighting. In total, the critical load consumes around 40% of the daily electricity demand [8], [29], which means an effective DR application could result in a considerable cost reduction. However, critical loads tend to be used in fixed periods based on consumer preferences. In this paper, only a small portion of critical loads are considered to participate in DR. Similarly, even though cold loads (e.g. appliances such as fridges and freezers) consume about 16% of the daily demand [29], consumers would still prefer to make free use of these over the entire day and not to commit to any predefined usage pattern.

2.1.2 Wet Load: Wet loads (e.g. dishwashers and washing machines) are normally classified as non-interruptible loads [30] in this type of studies since the directly-connected motor cannot complete a cycle instantly, and thus cannot participate in rapid-response DR schemes. However, since most of the current wet loads are equipped with a timer, users can set any starting time at off-peak time periods.

2.1.3 Heating and Hot Water: The direct heating load proposed in this analysis refers to the instant use of any heating appliance on demand, while in the storage heating scenario the boiler is switched on previously when the electricity tariff is low, and thus more appropriate for DR. Similarly, the use of DHW includes direct DHW and storage DHW. Within this context, the application of DHW on demand, i.e. direct DHW, is not considered suitable for DR as instantly changing the timing of hot water consumption would result in a high user weariness. As for the storage DHW, the water can be pre-heated at off-peak time periods and therefore it can be stored and used most effectively later.

2.1.4 Overload Fuse Capacity: In terms of protection to the HEMS, a maximum load limit needs to be set in case the sum power of all the appliances at time t is too large and may cause a trip in the system. The sum of $P_a(t)$ should be smaller than or equal to the fuse capacity F.

$$\sum_{a=1}^{A} P_a(t) \le F \quad \forall t \in \mathcal{T}, \forall a \in \mathcal{A} \tag{1}$$

2.1.5 Energy Storage System: The ESS in this study considers a power unit that is capable to store any excessive energy flow within the HEMS and discharge any required energy when mostly needed. Charging and discharging power $P^{ESS,c}(t)$ and $P^{ESS,d}(t)$ at each time slot are restricted by the maximum and minimum values as follow:

$$u^{ESS,c}(t)\underline{P}^{ESS,c} \le P^{ESS,c}(t) \le u^{ESS,c}(t)\overline{P}^{ESS,c}, \quad \forall t \in \mathcal{T} \tag{2}$$

$$u^{ESS,d}(t)\underline{P}^{ESS,d} \le P^{ESS,d}(t) \le u^{ESS,d}(t)\overline{P}^{ESS,d}, \quad \forall t \in \mathcal{T} \tag{3}$$

Binary variables are used to control the status of ESS.

$$u^{ESS,c}(t) + u^{ESS,d}(t) \le 1, \forall t \in \mathcal{T} \tag{4}$$

Regarding the state of charge (SOC) of the system, this is maintained within a specific range at all times over the day in (5), to provide the battery with a longer lifetime. In addition, as the analysis in this paper runs through a complete day period, the initial and final SOC states of the ESS are set to equal values in (6).

$$\underline{SOC} \le SOC(t) \le \overline{SOC}, \forall t \in \mathcal{T} \tag{5}$$

$$SOC(t=1) = SOC(t=48), \forall t \in \mathcal{T} \tag{6}$$

Where the SOC of ESS can be described as in (7) and (8). Either the charging or discharging power at time slot *t* can represent the energy at that specific time period. It should be noted that the charging efficiency is higher than the discharging efficiency for the analysis in this paper.

$$E^{ESS}(t) = E^{ESS}(t-1) + \eta^{ESS,c}P^{ESS,c}(t) - \eta^{ESS,d}P^{ESS,d}(t), \forall t \in \mathcal{T} \tag{7}$$

$$SOC(t) = E^{ESS}(t)/E^{ESS,total}, \forall t \in \mathcal{T} \tag{8}$$

Accordingly, the operation cost of ESS is yielded by the frequent charging and discharging over the entire daily time periods, which can be described as:

$$C^{ESS,total} = \sum_{t=1}^{T}[C^{ESS,unit}\eta^{ESS,c}P^{ESS,c}(t) + C^{ESS,unit}\eta^{ESS,d}P^{ESS,d}(t)] \quad \forall t \in \mathcal{T} \tag{9}$$

Where $C^{ESS,unit}$ can be represented by the ESS capital cost $C^{ESS,cap}$, its life cycle L^{ESS} and ESS capacity.

$$C^{ESS,unit} = C^{ESS,cap}/(2\,L^{ESS}E^{ESS,total}), \quad \forall t \in \mathcal{T} \tag{10}$$

2.1.6 Grid Energy Arbitrage: The HEMS is connected to the grid and the customer can purchase electricity at any time. Hence, determining the optimal electricity purchase time moment is important for saving operation cost. The following constraint defines the upper and lower limits for $P^b(t)$.

$$\underline{P^b} \le P^b(t) \le \overline{P^b}, \ \forall t \in \mathcal{T} \tag{11}$$

The equation below can represent the cost of buying energy, where $C^b(t)$ is the time-varying tariff.

$$C^{b,Total} = \sum_{t=1}^{T} C^b(t)P^b(t) \quad \forall t \in \mathcal{T} \tag{12}$$

2.1.7 HEMS Power Balance: A power balance constraint is used to ensure all the power supply sourced from the ESS, PV and energy purchase at time slot *t* is equal to the total power demand.

$$P^{ESS,d}(t) - P^{ESS,c}(t) + \omega^s(t) + P^b(t) = \sum_{a=1}^{A} P_a(t) \quad \forall t \in \mathcal{T}, \forall a \in \mathcal{A} \tag{13}$$

2.1.8 PV Generation: Based on historical data from PV generation, PV output forecast is required for the optimal application of HEMS [31, 32]. For that purpose, K-means clustering is applied in this paper by dividing a one year PV generation into sunny, cloudy and rainy days [33]. Then, based on the unique characteristic of each weather condition, artificial neural network (ANN) approach is used with known irradiance, ambient temperature and wind speed with back-propagation learning algorithm [34]. The forecast result is shown in Fig. 2, which shows the forecast and historical data approximately form a y=x regression line. Based on the forecast PV generation, the CCP expression is formulated. Equation (14) represents that the scheduled PV output exceeds a certain level at least chance of $1-\epsilon$ across the entire time horizon. The predefined upper level consists of the PV output forecast and uncertainty. It is considered to set the output higher the predefined value with a large probability

$1-\epsilon$, but lower than the predefined value with a large probability ϵ.

$$\Pr(\omega^s(t) \geq \omega^f(t) + \xi(t)) \geq 1-\epsilon, \forall t \in \mathcal{T} \quad (14)$$

2.2. Demand Response Implementation

TOU pricing scheme, as is presented in Fig. 4 [35], is applied containing peak, off-peak and super off-peak time periods, which encourages users to alter their consumption pattern voluntarily. Based on DR encouragement, load demand at each specific time slot could be reduced or shifted to other time slots. (15) describes the benefit of the user that participates in DR. The first term represents the reward because of certain load reduction $\Delta P_a^{re}(t)$. The second term represents the reward due to demand shifting $\Delta P_a^{sh}(t)$. (16) and (17) limit the load reduction and shifting respectively.

$$G^{DR} = \sum_{t=1,a=1}^{T,A} [R^{re}(t)\Delta P_a^{re}(t) + R^{sh}(t)\Delta P_a^{sh}(t)]$$

$$\forall t \in \mathcal{T}, \forall a \in \mathcal{A} \quad (15)$$

$$\underline{\Delta P_a^{re}}(t) \leq \Delta P_a^{re}(t) \leq \overline{\Delta P_a^{re}}(t), \forall t \in \mathcal{T}, \forall a \in \mathcal{A} \quad (16)$$

$$\underline{\Delta P_a^{sh}}(t) \leq \Delta P_a^{sh}(t) \leq \overline{\Delta P_a^{sh}}(t), \forall t \in \mathcal{T}, \forall a \in \mathcal{A} \quad (17)$$

The reward encouragement will result in cost reduction and load reduction that will benefit both customers and utilities. However, it will also bring weariness on DR when the accustomed behaviours of users will be altered due to DR schemes. The weariness function W^{DR} is therefore defined to evaluate the user weariness as presented in (18). W^{DR} is calculated by adding up the multiplication of weariness level (WL) and power deviation at each time slot of all appliances. Where the load reduction and load shifting of each appliance at each time slot $\Delta P_a(t)$ has its corresponding WL $\varphi_a^{re}(t)$ and $\varphi_a^{sh}(t)$, indicating that the WL varies depending on factor of time and appliance. In terms of time factor, WL values of all appliances are higher in peak time periods. As for appliance factor, the order of value for the WL factor of appliances is 'critical load' > 'heating' = 'DHW' > 'wet'. DR of cold load is not involved in this analysis.

$$W^{DR} = \sum_{t=1,a=1}^{T,A} \varphi_a^{re}(t)\,\Delta P_a^{re}(t) + \varphi_a^{sh}(t)\,\Delta P_a^{sh}(t)$$
$$\forall t \in \mathcal{T}, \forall a \in \mathcal{A} \quad (18)$$

2.3. HEMS Objective function

When DR is not applied in HEMS, the only objective is to determine the most economic result, while DR is being applied, both economic and weariness objectives will be considered because the impact of DR on user weariness cannot be ignored.

$$M = C^{b,Total} + C^{ESS,total} - G^{DR} \quad (19)$$
$$Obj = min[\lambda^{DR} M + (1-\lambda^{DR}) W^{DR}] \quad (20)$$

Therefore, to jointly optimize the objectives from both cost of HEMS and user weariness, the weighting factor of DR (denoted as λ^{DR}) is required to effectively represent the weight of weariness in the overall objective. The objective function is denoted as *Obj*, which includes both economic sub objective M and weariness sub objective W^{DR}. The economic sub objective *M* includes cost of energy purchase and ESS degradation, minus any benefit arising from DR actions. While weariness sub objective W^{DR} considers the implicit DR weariness from demand reduction or shifting.

3. Methodology

The optimization problem defined in this paper for application in HEMS must be solved by considering the uncertain solar generation and complex chance constrained formulation. Accordingly, common methods to handle the solar generation uncertainty on HEMS are either RO or CCP [14], [36]. In RO, the uncertainty set is easier to estimate only based on forecast data, but the drawback is the over-conservativeness when the worst case lies on bounds with low probability. On the other hand, CCP coping with a large number of uncertainty samples is computationally demanding. And analytical reformulation is normally over-optimistic when fitting the historical data to a specific uncertainty distribution.

3.1. Distributionally Robust Reformulation for CCP

As opposed to the previous methods, with DRO, neither making assumptions on uncertainty distributions nor a large number of uncertainty samples are required, but it only requires limited statistical information such as moment information. Compared with CCP, DRO provides an ambiguity set that considers all the possible distributions rather than making assumptions on a certain distribution of CCP. Compared with RO, DRO considers the worst distribution to reduce conservatism rather than the worst case on its own [18, 19]. The ambiguity set is defined by incorporating moment information such as mean and covariance, which considers all the possible distributions.

Regarding the RE power output within HEMS (i.e. from PV), a time varying lower bound $\omega^f(t) + \xi(t)$ is set to ensure PV generation at each time slot is above a certain level.

$$\tilde{A}_i(\xi_i)x \geq \tilde{b}_i(\xi_i) = \{\omega^s(t) \geq \omega^f(t) + \xi(t)\} \quad (21)$$

$\tilde{A}_i$ is used to represent the ith row of the random matrix $\tilde{A}$ and deterministic b_i is used to represent the ith element of vector b. The chance constraint i is satisfied with probability 1-ϵ_i. In other words, it also means under chance of ϵ_i, the constraint cannot be satisfied.

$$\Pr\left(\tilde{A}_i(\xi_i)x \geq \tilde{b}_i(\xi_i)\right) \geq 1-\epsilon_i \quad (22)$$

ξ_i is the random variable that affects constraint i. $\tilde{A}_i$ can be represented by $\tilde{A}_i(\xi_i)$ that is defined as the affine function including deterministic part A_{i0} and uncertain part $A_{ik}\,\xi_{ik}$ [37, 38], where K is the dimension of ξ_i.

$$\tilde{A}_i(\xi_i) = A_{i0} + \sum_{k=1}^{K} A_{ik}\,\xi_{ik} \quad (23)$$

$$\tilde{b}_i(\xi_i) = b_{i0} + \sum_{k=1}^{K} b_{ik}\,\xi_{ik} \tag{24}$$

Then two vectors are formulated and will be used in the later reformulation content, $\bar{A}_i^x = \langle b_{i1} - A_{i1}x, b_{i2} - A_{i2}x, \dots b_{ik} - A_{iK}x \rangle$ and $\bar{b}_i^x = A_{i0}x - b_{i0}$. The ambiguity set D with the first and second moment information can be described as:

$$D = \left\{ f(\xi) \middle| \begin{cases} \mathrm{P}\{f(\xi)\} = 1 \\ \mathrm{E}\{\xi\} = \mu + \gamma_1 \\ \mathrm{E}\{(\xi - \mu)\cdot(\xi - \mu)^{\mathrm{T}}\} = \gamma_2 \Gamma \end{cases} \right\} \tag{25}$$

In this paper, the mean vector and covariance matrix are considered as the moment information and DRO is used to reformulate CCP to a tractable SOCP problem. Robustness is reflected on parameters γ_1 and γ_2 that can be altered and therefore be used to decide the size of the ambiguity set. Larger values of γ_1 and γ_2 result in more robust results [18]. Accordingly, $\gamma_1 = 0$ and $\gamma_2 = 1$ that are commonly used in research are used in this paper, also considering $D' \subset D$. Hence, the ambiguity set for each chance constraint i is provided by equation (26).

$$D' = \left\{ f(\xi) \middle| \begin{cases} \mathrm{P}\{f(\xi)\} = 1 \\ \mathrm{E}\{\xi\} = \mu_0 \\ \mathrm{E}\{(\xi - \mu_0)\cdot(\xi - \mu_0)^{\mathrm{T}}\} = \Gamma_0 \end{cases} \right\} \tag{26}$$

The uncertainty is reflected on the random ξ matrix, which consists of elements in J rows and K columns. Thus, $\xi_i^{j,k}$ is an element at jth row and kth column. To construct the ambiguity set, the mean and covariance matrices are required. The covariance value for $\xi^{j,k}$ can be calculated as:

$$\Gamma_i^{j,k} = E\{\,\xi_i^j - E[\xi_i^j])(\xi_i^k - E[\xi_i^k])\} \tag{27}$$

Hence, the distributionally robust constraint i in (21) can be rewritten as:

$$\inf_{f(\xi)\in D, \xi\sim(\mu_0,\Gamma_0)} \mathrm{P}\left((\bar{A}_i^x)^{\mathrm{T}}\xi - \bar{b}_i^x \geq 0\right) \geq 1 - \epsilon_i \tag{28}$$

Which can be further reformulated to the following constraint:

$$\sup_{f(\xi)\in D, \xi\sim(\mu_0,\Gamma_0)} \mathrm{P}\left((\bar{A}_i^x)^{\mathrm{T}}\xi - \bar{b}_i^x \geq 0\right) \leq \epsilon_i \tag{29}$$

According to the tight multivariate single sided Chebyshev bound [39] and the SOCP reformulation by [40], a random variable y, with known mean μ and variance σ, can be expressed as:

$$\mathrm{P}(\mathrm{y} \geq (1+m)\mu) = \frac{\sigma}{\sigma + \mu^2 m^2} \tag{30}$$

Where m is a constant between 0 and 1. In (30), m is given by:

$$m = \frac{\bar{b}_i^x}{(\bar{A}_i^x)^{\mathrm{T}}\mu_0} - 1 \tag{31}$$

Table 1 Parameters of HEMS

System parameters	
ESS	$\underline{P}^{ESS,c}$=$\underline{P}^{ESS,d}$=0, $\overline{P}^{ESS,c}$=$\overline{P}^{ESS,d}$=4.8kW
	$\underline{SOC}$=30%, $\overline{SOC}$=90%, $\eta^{ESS,c}$=$\eta^{ESS,d}$=0.88
	$C^{ESS,unit}$=0.0042 p.u./kW, $E^{ESS,total}$=4.8kWh
Electricity purchase	$\underline{P}^{b}$=0, $\overline{P^{b}}$=4kW
PV	Capacity=1kW

Then, equation (29) is equivalent to:

$$\sup_{f(\xi)\in D, \xi\sim(\mu_0,\Gamma_0)} \mathrm{P}\{\,\xi^{\mathrm{T}}\bar{A}_i^x > b_i\} = \frac{\bar{A}_i^{x\mathrm{T}}\Gamma_0\,\bar{A}_i^x}{\bar{A}_i^{x\mathrm{T}}\Gamma_0\,\bar{A}_i^x + {\mu_0}^{\mathrm{T}^2} m^2} \tag{32}$$

$$\sqrt{\bar{A}_i^{x\mathrm{T}}\Gamma_0\,\bar{A}_i^x} \leq \sqrt{\frac{\epsilon_i}{1-\epsilon_i}}\,(\,\bar{b}_i^x - {\mu_0}^{\mathrm{T}}\bar{A}_i^x) \tag{33}$$

Therefore, when the DRCCP approach is applied to the PV power output within HEMS, it makes sure that at each particular time slot, at least chance $1 - \epsilon_i$ the output can be larger than the predefined lower bound. Overall, it also ensures the total PV output is larger than the predefined total output value for the entire operation time horizon. Thus, the equation (34) below can be applied in both DRCCP and CCP for performance comparison.

$$\Pr(\omega^s(t) \geq \omega^f(t) + \xi(t)) \geq 1 - \epsilon\,,\ \forall t \in \mathcal{T} \tag{34}$$

3.2. Overall DRCC-HEMS Approach

Based on all previous assumptions, the step-by-step methodology applied on DRCC-HEMS is described as follows:

i. Acquire data: decomposed residential load, solar generation, ESS specifications and TOU pricing scheme.
ii. Cluster solar generation into three categories in terms of weather conditions and apply forecast.
iii. Formulate constraints and objective for HEMS and set a chance constraint for solar generation.
iv. Construct ambiguity set and apply distributionally robust formulation for CCP through (21)-(33).
v. Solve the DRCC-HEMS by an efficient commercial solver.

4. Performance Evaluation

This section presents the resulting analysis from the HEMS performance. Firstly, a HEMS configuration is proposed, followed by the PV forecast which provides the raw information required to construct the ambiguity set. The DRCC-HEMS is then solved considering DR and comparisons on appliance scheduling and operation curves are discussed. DRCCP is also compared with CCP method. As a result, the overall HEMS objective is optimized, and the sub-objectives incorporating operation cost and weariness function are separately analysed and discussed. It must be noted that all outcome results regarding the daily operation cost of HEMS is expected overall cost. All numerical simulations are solved by CPLEX 12.8 with Intel i7-7700 CPU, 3.6 GHz and 16 GB RAM.

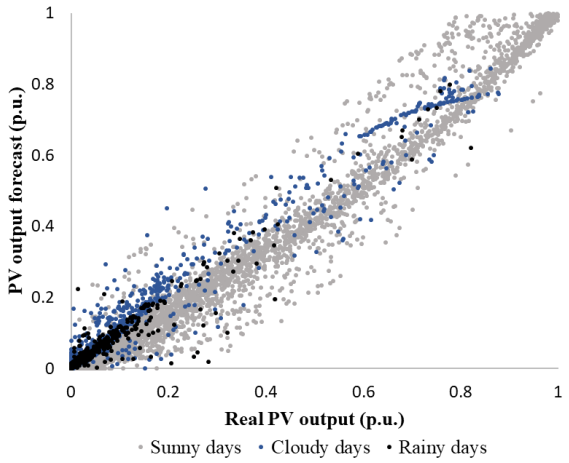

Fig. 2. *PV output forecast for application with HEMS*

4.1. HEMS Setup

As presented in Fig. 1, the HEMS structure proposed in this paper was originally designed and deployed for SoLa BRISTOL Project [41] in the city of Bristol (UK), and is currently tested in the Smart Grid Laboratory at the University of Bath. A PV generator with a DC/DC converter and a battery set are connected to a common DC bus, supplying the daily energy demand to a domestic load emulator through an AC/DC inverter. The technical parameters are shown in Table 1 [35, 41, 42], and the base case confidence interval of CC is set as 1- ϵ =95%. Regarding the onsite RE generation, the PV output data is recorded annually at the University premises. The forecast error was originally normal distributed approximately, which is then fitted to be perfectly normal distributed. As described in section 2, rather than using historical data directly, the forecast PV output is used as the source of information for building the ambiguity set in the HEMS optimization. The ANN forecast result which corresponds to this analysis is shown in Fig. 2.

4.2. Numerical Results

Firstly, five DR scenarios, with different DR factors representing diverse customer preferences on cost saving and weariness function are applied for the optimal performance of HEMS. The DR scheme with weighting factor λ^{DR}=0.5 is considered as the base case, and both cost and weariness are therefore set as 1 p.u. As compared to the base case, three typical DR scenarios, with λ^{DR} =0, 0.5 and 1 are denoted as scenario 1, 2 and 3 respectively. Secondly, the optimal home appliance scheduling after the application of both DR and DRCCP for scenarios 1, 2 and 3 are directly compared and presented. Finally, this section presents the optimal electricity purchase and SOC curves.

Based on the previous assumptions, Table 2 presents five different scenarios, which are distinguished by five different sets of λ^{DR} and therefore define the diversity in customer preferences on cost saving and weariness function. As expected, and as shown in Table 2, the resulting HEMS operation cost is reduced as soon as any DR participation is considered for the HEMS users (i.e. $\lambda^{DR} > 0$). On the contrary, the user weariness increases accordingly with the rise of λ^{DR}.

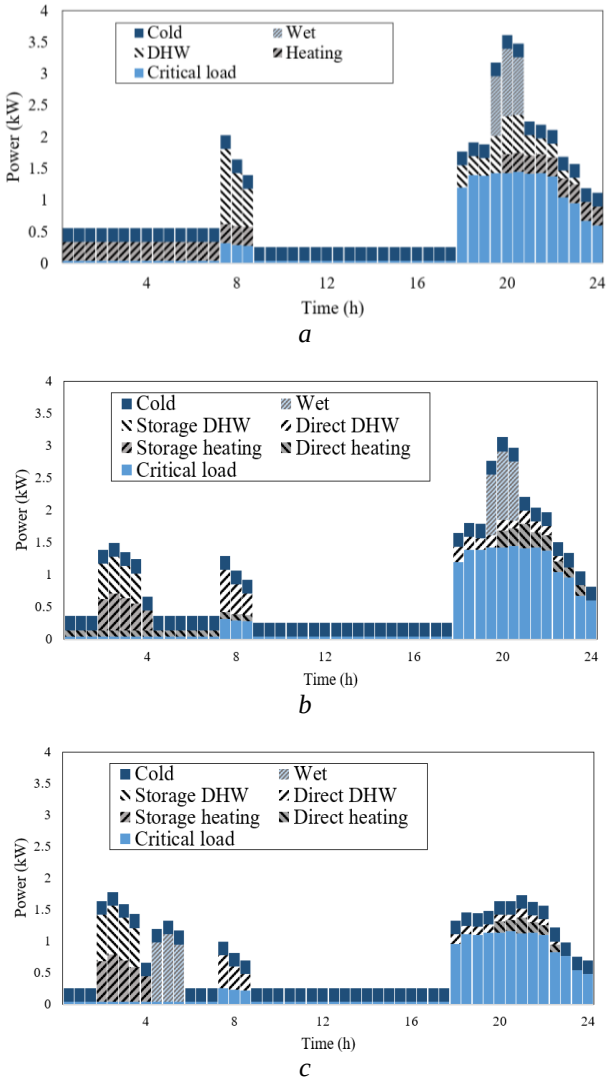

Fig. 3. *Appliance scheduling curve for HEMS optimization:*

(a) $\lambda^{DR} = 0$, **(b)** $\lambda^{DR} = 0.5$, **(c)** $\lambda^{DR} = 1$

The two extremes occur when λ^{DR} is equal to 0, i.e. when DR is not applied at all, and 1, when DR is fully implemented.

Fig. 3(a) presents the original power consumption of all home appliances in a typical household without any DR intervention (i.e. $\lambda^{DR} = 0$). Unlike the average after-diversity demand (ADD) concept, which reflects the overall energy consumption of many domestic users, the consumption pattern considered for analysis in Fig. 3 represents a single individual household with a typical 'working-pattern' behaviour (i.e. electricity users get off home at 9:00 in the morning and return home at 18:00 in the evening). A short-period peak demand takes place during the morning when there is high on-demand consumption of DHW appliances. Another long-period peak demand occurs from 18:00, when critical and DHW loads are mostly consumed, followed by the highest peak demand when wet and heating loads are added into the overall consumption.

After the application of DR on HEMS (i.e. $\lambda^{DR} > 0$), the load consumption is presented for scenario 2 in Fig. 3(b) with $\lambda^{DR} = 0.5$, which means the DR strategy considers equally important the daily operation cost of HEMS and the user weariness. The initial DHW and heating loads are divided into: i) storage DHW and heating when hot water and

Table 2 Cost and Weariness effect from different λ^{DR}

λ^{DR}	Cost (p.u.)	Weariness (p.u.)
0	1.30	0.00
0.25	1.14	0.43
0.5	1.00	1.00
0.75	0.91	1.85
1	0.83	2.97

heat can be stored during off-peak periods and used later, and ii) direct DHW and heating when users tend to consume DHW and heating immediately. As shown in Fig. 3(b) for scenario 2, the highest peak demand in the evening (i.e. from 19:30 to 20:30) is reduced by 14% and shifted into the night between 2:00 and 4:00. This creates a new peak of 92% increase when storage DHW and heating are used for storing water and heat for later use. In addition, the consumption from the 19:30-20:30 peak is decreased due to the 54% shift of storage DHW. Apart from the great impact on peak demand because of DR, the overall load consumption is reduced by 7% through reducing a small amount of demand at every time slot.

Finally, if the DR intervention simply considers saving energy cost as the objective function, thus ignoring weariness (i.e. λ^{DR} = 1), the resulting load curve after HEMS optimisation is shown for scenario 3 in Fig. 3(c). The biggest difference from scenario 2 is the wet load shift from 19:30-20:30 to 4:30-5:30. Additionally, heating and DHW loads are further shifted and aggregated to the time period 2:00-4:00 in order to switch them off at other time slots and save standby energy consumption. Also, since λ^{DR} is at its highest value, consumption of all the appliance types is further reduced at every time period. Overall, compared with scenario 1 and 2, 24% and 17% of the total electricity demand is reduced respectively.

Apart from the best-fitted appliance consumption, in Fig. 5, the operation of HEMS also results in an optimal power scheduling curve for the SOC of ESS and energy purchase, including DR scenarios 1,2 and 3 for three different weather conditions (sunny, cloudy and rainy). As previously discussed, the TOU tariff is presented in Fig. 4, which is an essential factor for the optimal power scheduling with HEMS. Alternatively, the SOC of ESS and energy purchase from the grid largely depend on weather conditions, which is reflected in Fig. 5 by the similar power scheduling curves resulting for each weather condition. As a general comparison, in cloudy days, the ESS is required to produce about 7% and 21% more energy than in sunny and rainy days. On the other hand, the amount of buying electricity on sunny days is 22% and 53% less than in cloudy and rainy days respectively. In scenario 1, with no DR intervention at all (i.e. λ^{DR} = 0), an increase of 9% and 25% in electricity purchase occurs due to higher energy consumption, as compared with scenarios 2 and 3 respectively.

For example, in scenario 2 (λ^{DR} = 0.5), since a large amount of appliance consumption is shifted to the period 2:00-4:00, an intensive electricity purchase is required without discharging the battery. Then, due to the demand increase between 7:30 and 8:30 in the morning, ESS is slightly discharged until when PV starts to harness power again at 8:00. The battery is assumed to be charging at all times when the PV is generating and there is no demand from HEMS. Because of the high energy consumption during the

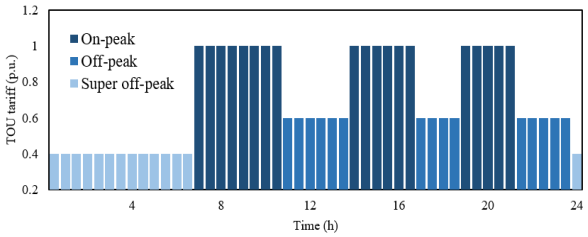

Fig. 4. *Daily TOU tariff for HEMS application*

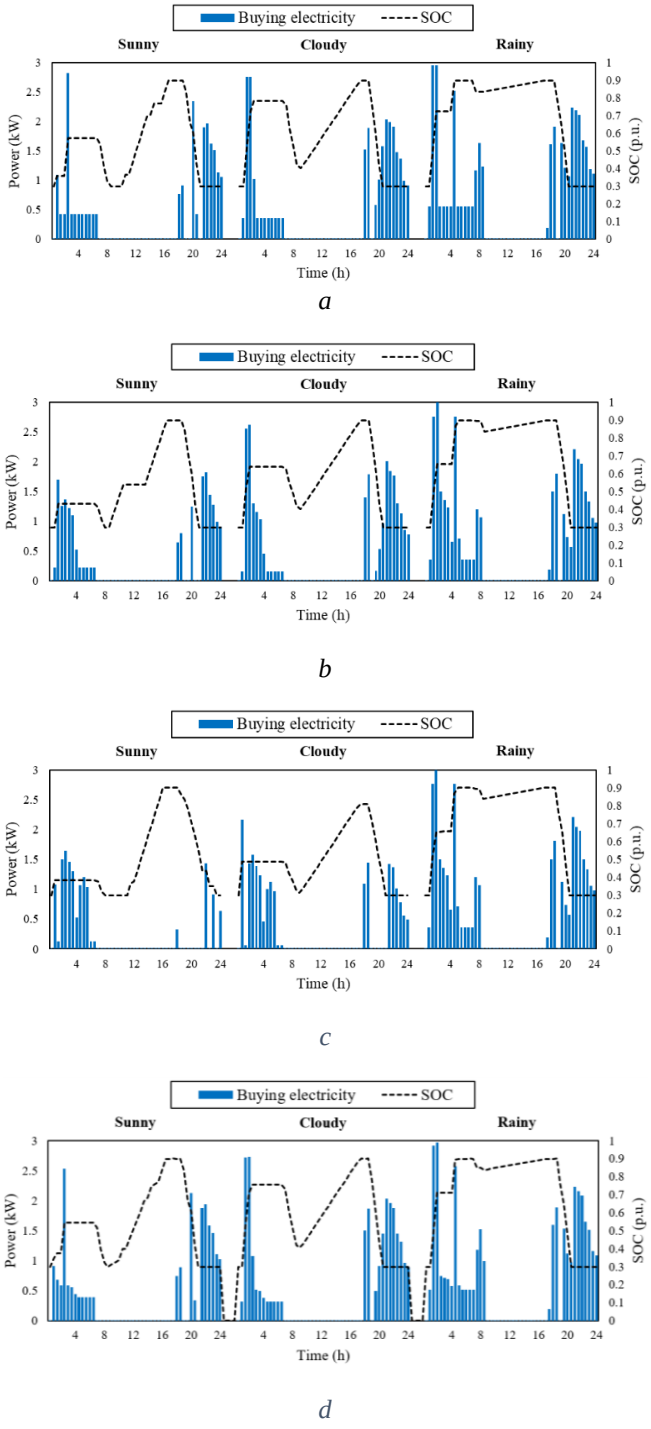

Fig. 5. *Buying electricity scheduling and SOC curve for:*

(a) λ^{DR} = 0, **(b)** λ^{DR} = 0.5, **(c)** λ^{DR} = 1, **(d)** λ^{DR} = 0.07

Table 3 Comparison of expected cost and CPU time for three DR scenarios (1- ϵ = 95%)

		DRCCP	CCP	Deterministic
λ^{DR} = 0	Cost (p.u.)	1.30	1.24	1.22
	CPU time (s)	0.03	8.80	0.03
λ^{DR} = 0.5	Cost (p.u.)	1.00	0.97	0.94
	CPU time (s)	0.03	6.84	0.03
λ^{DR} = 1	Cost (p.u.)	0.83	0.78	0.76
	CPU time (s)	0.02	4.75	0.02

evening peak time, ESS is accordingly discharged all the way from the highest SOC of 90% to the lowest SOC value of 30%. Therefore, the energy purchased individually supplies the HEMS demand from 21:30 to 00:00. A similar power scheduling is yielded in cloudy days, however with a larger electricity purchase due to a lower availability from the PV generation. With the increased demand shift to morning times, more buying electricity is needed on rainy days, with a rapid charging required from the battery. In that case, due to the lack of sufficient PV output during the day, the battery is barely used (neither to charge nor to discharge) and SOC is kept around 90% for 14 hours during the day time.

In order to find out the optimal objective that fulfils both daily operation cost and weariness. Instead of considering as a fixed coefficient for sub objectives, λ^{DR} is considered as a decision variable to determine the overall optimal objective. Calculation is made and the optimal result is yielded when $\lambda^{DR} = 0.07$. Accordingly, the SOC and electricity purchase curves are shown in Fig. 5(c). According to the resulting λ^{DR}, it can be found that the optimum exists when slight concentration is on operation cost while large concentration is on weariness. The weighting factor can be adjusted by the HEMS operators depending on the customer's preference on cost saving or weariness.

4.3. Performance Comparison with CCP

In this section, the performance of DRO (i.e. the proposed DRCCP technique) and the benchmark approach (scenario approach) to solve the CC-HEMS problem is analysed by comparing the resulting daily operation cost and computation time to solve HEMS optimization. Moreover, as an additional comparison, a deterministic optimization approach is investigated without considering any uncertainty from the PV generation. In particular, the benchmark approach CCP uses a scenario approximation, with a large set of scenarios, where ϵ of scenarios violates the constraint (31) but the rest adheres. The dimensionality of the analysis is addressed by scenario reduction by comparing moment information that includes expectation, variance, skewness and kurtosis. In Table 3, the resulting costs (in per unit values) and computation time are compared when DRCCP, CCP and deterministic optimization are all applied in sunny conditions, with a confidence level of 1- ϵ =95%. When λ^{DR}=0.5, the cost of DRCCP is considered as base case and set as 1 p.u.

As compared in Table 3, both DRCCP and deterministic optimization analyses require less CPU time as compared with CCP, which needs to consider a wide range of scenarios. Regarding the cost, as no uncertainty from PV generation is concerned, deterministic optimization with a fixed PV output yields more optimistic results than CCP and DRCCP, which also include the probabilities of PV generation varying under a fixed maximum value. In spite of the improvement in CPU time, the comparison in Table 3 also demonstrates that DRCCP results in a more conservative solution than CCP (which requires a high computation burden), reflecting on a more conservative PV generation and a higher operation cost. With the increase of the DR weighting factor (i.e. $\lambda^{DR} > 0$), more DR involved results in a lower cost and less CPU time due to a more efficient and economical electricity consumption pattern and a reduced load demand. Overall, DRCC-HEMS saves computation time as compared with CCP and incorporates the implicit uncertainty from PV generation as compared with deterministic optimization. The scenario-based CC-HEMS yields a reliable result considering uncertainty but requires much more computation complexity. While the deterministic HEMS results in a more optimistic result solely considering the fixed higher values of PV generation but ignoring lower generation in probability ϵ.

Table 4 Expected cost for DRCCP and CCP with different confidence levels

	Cost (p.u.)	
ϵ	DRCCP	CCP
1%	0.994	0.970
2%	0.996	0.973
3%	0.999	0.975
4%	1.000	0.976
5%	1.000	0.977
6%	1.000	0.978
7%	1.007	0.984
8%	1.011	0.989
9%	1.012	0.991
10%	1.012	0.993

Finally, in Table 4, a cost comparison is provided when DRCCP and CCP techniques are applied to solve the HEMS problem with different values of confidence level ϵ. As rthe eference, when ϵ is 5%, the cost of DRCCP is considered as the base case and set as 1 p.u. Although ϵ =5% is mostly studied in the proposed CC problem in this paper, the impact on the daily HEMS operation cost by changing the confidence level ϵ from 1% to 10% is also investigated. As shown in Table 4, When ϵ grows, the confidence interval $1 - \epsilon$ decreases, which means it is less probable that the scheduled PV power is larger than the predefined level. Accordingly, the event of output exceeding violation is less frequent. Thus, with the increase of ϵ, the overall scheduled PV output is becoming smaller. Accordingly, CCP results in an average 2% reduced operation cost for HEMS. The cost difference generally reduces when ϵ increases, which is a direct effect from a less strict control on minimum PV generation. In general, DRCCP yields more conservative results than the CCP. It offers large savings in the computation burden, similar to those obtained with the use of deterministic optimization.

4.4. Discussion on Numerical Results

The classical scenario approximation is used to solve CC-HEMS in comparison with DRCCP, which is fully described in terms of computation time and daily operation cost from the HEMS. The resulting difference among the three scenarios shows that the DRCC-HEMS alters energy consumption patterns in a great extent through load curtailment and demand shifting. Thus, by implementing the DRCC-HEMS approach, with full consideration of solar energy uncertainty, a significant reduction in customer electricity bills can be achieved, as well as a faster system response due to the reduced complexity in the computation of results. The analysis shows that the advantage of DRCC-HEMS can be listed:

1. Protecting information privacy: In practice, acquiring the full knowledge of uncertainty is not always possible. Gathering the PV usage data from HEMS customers is even not practical. A large data set requires the participation of customers by sharing their PV usage information, which inevitably violates the privacy of customers. DRCC-HEMS does not require the use of large uncertainty samples, but only moment information obtained from limited data, thus protecting customer privacy.
2. Computationally efficient: Conventional CC-HEMS requires large data sets by using detailed distribution modelling and then transforms them into deterministic models to solve by sophisticated mathematical techniques. By contrast, DRCC-HEMS is more computational efficient which only needs moment information.
3. Accurate costs: In CC-HEMS, when the dataset is not sufficiently large, assigning a specific probability distribution to uncertain renewable generation will cause big errors. By contrast, DRCC-HEMS provides customers a more accurate scheduling plan by reliable moment information.
4. Considering uncertainties: Compared to the deterministic HEMS, although it produces lower results, the PV uncertainty is ignored, which in reality is not practical to be considered as deterministic datasets. However, these uncertainties can be easily included in the developed DRCC-HEMS. By implementing the DRCC-HEMS approach, with the full consideration of solar energy uncertainty, a significant reduction in customer electricity bills can be achieved, as well as a faster system because of the reduced complexity in modelling.

5. Conclusion

In this paper, the optimal performance of a hybrid PV-storage HEMS is investigated with precise control on ESS, electricity purchase from the grid, specific domestic appliances for DR, as well as considering the uncertainty from PV generation. In order to solve the HEMS problem, different DR interventions are studied for energy cost reduction by altering customer consumption patterns. The uncertainty arising from solar energy (i.e. the ambiguity set) is fully incorporated into the HEMS by applying DRCCP, which no longer require the use of inaccurate probability distributions associated with uncertainty.

Overall, it is concluded that the DRCCP presented in this paper, in combination with all the parameters considered for an optimal HEMS performance, provides the best solution for the analysis and application of DR at residential customer level, which at the same time fully acknowledges the uncertainty arising from any type of RE generation, as proven for a hybrid PV-storage HEMS.

6. References

[1] C. Chen, S. Duan, T. Cai, B. Liu, and G. Hu, "Smart energy management system for optimal microgrid economic operation," *IET Renewable Power Generation,* vol. 5, pp. 258-267, 2011.

[2] H. Kanchev, D. Lu, F. Colas, V. Lazarov, and B. Francois, "Energy Management and Operational Planning of a Microgrid With a PV-Based Active Generator for Smart Grid Applications," *IEEE Transactions on Industrial Electronics,* vol. 58, pp. 4583-4592, 2011.

[3] S. S. S. R. Depuru, L. Wang, V. Devabhaktuni, and N. Gudi, "Smart meters for power grid—Challenges, issues, advantages and status," in *2011 IEEE/PES Power Systems Conference and Exposition*, 2011, pp. 1-7.

[4] P. Tarasak, C. C. Chai, Y. S. Kwok, and S. W. Oh, "Demand Bidding Program and Its Application in Hotel Energy Management," *IEEE Transactions on Smart Grid,* vol. 5, pp. 821-828, 2014.

[5] M. A. F. Ghazvini, P. Faria, S. Ramos, H. Morais, and Z. Vale, "Incentive-based demand response programs designed by asset-light retail electricity providers for the day-ahead market," *Energy,* vol. 82, pp. 786-799, 2015.

[6] M. Pipattanasomporn, M. Kuzlu, and S. Rahman, "An Algorithm for Intelligent Home Energy Management and Demand Response Analysis," *IEEE Transactions on Smart Grid,* vol. 3, pp. 2166-2173, 2012.

[7] Z. Chen, L. Wu, and Y. Fu, "Real-Time Price-Based Demand Response Management for Residential Appliances via Stochastic Optimization and Robust Optimization," *IEEE Transactions on Smart Grid,* vol. 3, pp. 1822-1831, 2012.

[8] I. Joo and D. Choi, "Optimal household appliance scheduling considering consumer's electricity bill target," *IEEE Transactions on Consumer Electronics,* vol. 63, pp. 19-27, 2017.

[9] Y. Xiang, J. Liu, and Y. Liu, "Robust Energy Management of Microgrid With Uncertain Renewable Generation and Load," *IEEE Transactions on Smart Grid,* vol. 7, pp. 1034-1043, 2016.

[10] A. Hussain, V. H. Bui, and H. M. Kim, "Robust Optimal Operation of AC/DC Hybrid Microgrids Under Market Price Uncertainties," *IEEE Access,* vol. 6, pp. 2654-2667, 2018.

[11] F. Y. Melhem, O. Grunder, Z. Hammoudan, and N. Moubayed, "Energy Management in Electrical Smart Grid Environment Using Robust Optimization Algorithm," *IEEE Transactions on Industry Applications,* vol. 54, pp. 2714-2726, 2018.

[12] J. Liu, H. Chen, W. Zhang, B. Yurkovich, and G. Rizzoni, "Energy Management Problems Under

Uncertainties for Grid-Connected Microgrids: A Chance Constrained Programming Approach," *IEEE Transactions on Smart Grid*, vol. 8, pp. 2585-2596, 2017.
[13] Z. Wu, W. Gu, R. Wang, X. Yuan, and W. Liu, "Economic optimal schedule of CHP microgrid system using chance constrained programming and particle swarm optimization," in *2011 IEEE Power and Energy Society General Meeting*, 2011, pp. 1-11.
[14] Y. Huang, L. Wang, W. Guo, Q. Kang, and Q. Wu, "Chance Constrained Optimization in a Home Energy Management System," *IEEE Transactions on Smart Grid*, vol. 9, pp. 252-260, 2018.
[15] W. Wei, F. Liu, and S. Mei, "Distributionally Robust Co-Optimization of Energy and Reserve Dispatch," *IEEE Transactions on Sustainable Energy*, vol. 7, pp. 289-300, 2016.
[16] P. Xiong, P. Jirutitijaroen, and C. Singh, "A Distributionally Robust Optimization Model for Unit Commitment Considering Uncertain Wind Power Generation," *IEEE Transactions on Power Systems*, vol. 32, pp. 39-49, 2017.
[17] Z. Wang, Q. Bian, H. Xin, and D. Gan, "A Distributionally Robust Co-Ordinated Reserve Scheduling Model Considering CVaR-Based Wind Power Reserve Requirements," *IEEE Transactions on Sustainable Energy*, vol. 7, pp. 625-636, 2016.
[18] E. Delage and Y. Ye, "Distributionally robust optimization under moment uncertainty with application to data-driven problems," *Operations research*, vol. 58, pp. 595-612, 2010.
[19] J. Goh and M. Sim, "Distributionally robust optimization and its tractable approximations," *Operations research*, vol. 58, pp. 902-917, 2010.
[20] Z. Hu and L. J. Hong, "Kullback-Leibler divergence constrained distributionally robust optimization," *Available at Optimization Online*, 2013.
[21] P. M. Esfahani and D. Kuhn, "Data-driven distributionally robust optimization using the Wasserstein metric: Performance guarantees and tractable reformulations," *Mathematical Programming*, vol. 171, pp. 115-166, 2018.
[22] C. Wang, R. Gao, W. Wei, M. Shafie-khah, T. Bi, and J. P. S. Catalao, "Risk-based Distributionally Robust Optimal Gas-Power Flow With Wasserstein Distance," *IEEE Transactions on Power Systems*, pp. 1-1, 2018.
[23] Y. Chen, Q. Guo, H. Sun, Z. Li, W. Wu, and Z. Li, "A Distributionally Robust Optimization Model for Unit Commitment Based on Kullback–Leibler Divergence," *IEEE Transactions on Power Systems*, vol. 33, pp. 5147-5160, 2018.
[24] Z. Shi, H. Liang, S. Huang, and V. Dinavahi, "Distributionally Robust Chance-Constrained Energy Management for Islanded Microgrids," *IEEE Transactions on Smart Grid*, pp. 1-1, 2018.
[25] W. Xie and S. Ahmed, "Distributionally Robust Chance Constrained Optimal Power Flow with Renewables: A Conic Reformulation," *IEEE Transactions on Power Systems*, vol. 33, pp. 1860-1867, 2018.
[26] Y. Zhang, S. Shen, and J. L. Mathieu, "Distributionally Robust Chance-Constrained Optimal Power Flow With Uncertain Renewables and Uncertain Reserves Provided by Loads," *IEEE Transactions on Power Systems*, vol. 32, pp. 1378-1388, 2017.
[27] Z. Wen, D. O'Neill, and H. Maei, "Optimal Demand Response Using Device-Based Reinforcement Learning," *IEEE Transactions on Smart Grid*, vol. 6, pp. 2312-2324, 2015.
[28] C. Vivekananthan, Y. Mishra, G. Ledwich, and F. Li, "Demand Response for Residential Appliances via Customer Reward Scheme," *IEEE Transactions on Smart Grid*, vol. 5, pp. 809-820, 2014.
[29] "The impact of changing energy use patterns in buildings on peak electricity demand in the UK," B. R. Establishment, Ed., ed, 2011.
[30] J. Yang, J. Liu, Z. Fang, and W. Liu, "Electricity scheduling strategy for home energy management system with renewable energy and battery storage: a case study," *IET Renewable Power Generation*, vol. 12, pp. 639-648, 2018.
[31] O. Abedinia, D. Raisz, and N. Amjady, "Effective prediction model for Hungarian small-scale solar power output," *IET Renewable Power Generation*, vol. 11, pp. 1648-1658, 2017.
[32] N. Amjady and O. Abedinia, "Short Term Wind Power Prediction Based on Improved Kriging Interpolation, Empirical Mode Decomposition, and Closed-Loop Forecasting Engine," *Sustainability*, vol. 9, p. 2104, 2017.
[33] T. Kanungo, D. M. Mount, N. S. Netanyahu, C. D. Piatko, R. Silverman, and A. Y. Wu, "An efficient k-means clustering algorithm: Analysis and implementation," *IEEE Transactions on Pattern Analysis & Machine Intelligence*, pp. 881-892, 2002.
[34] A. Mellit and A. M. Pavan, "A 24-h forecast of solar irradiance using artificial neural network: Application for performance prediction of a grid-connected PV plant at Trieste, Italy," *Solar Energy*, vol. 84, pp. 807-821, 2010.
[35] P. Tian, X. Xiao, K. Wang, and R. Ding, "A Hierarchical Energy Management System Based on Hierarchical Optimization for Microgrid Community Economic Operation," *IEEE Transactions on Smart Grid*, vol. 7, pp. 2230-2241, 2016.
[36] C. Wang, Y. Zhou, B. Jiao, Y. Wang, W. Liu, and D. Wang, "Robust optimization for load scheduling of a smart home with photovoltaic system," *Energy Conversion and Management*, vol. 102, pp. 247-257, 2015.
[37] A. Shapiro, D. Dentcheva, and A. Ruszczyński, *Lectures on stochastic programming: modeling and theory*: SIAM, 2009.
[38] S. Zymler, D. Kuhn, and B. Rustem, "Distributionally robust joint chance constraints with second-order moment information," *Mathematical Programming*, vol. 137, pp. 167-198, 2013.
[39] D. Bertsimas and I. Popescu, "Optimal inequalities in probability theory: A convex optimization approach," *SIAM Journal on Optimization*, vol. 15, pp. 780-804, 2005.
[40] M. R. Wagner, "Stochastic 0–1 linear programming under limited distributional information," *Operations Research Letters*, vol. 36, pp. 150-156, 2008.
[41] C. Zhao, S. Dong, C. Gu, F. Li, Y. Song, and N. P. Padhy, "New Problem Formulation for Optimal

Demand Side Response in Hybrid AC/DC Systems," *IEEE Transactions on Smart Grid*, vol. PP, pp. 1-1, 2016.

[42] A. Ghasemi, M. Banejad, and M. Rahimiyan, "Integrated energy scheduling under uncertainty in a micro energy grid," *IET Generation, Transmission & Distribution*, vol. 12, pp. 2887-2896, 2018.